Journal of Alloys and Compounds, 190 (1993) 273–277
JALCOM 461

Studies on local structure in hydrogenated amorphous $LaNi_{5.0}$ films using extended X-ray absorption fine structure

Tomoyoshi Suenobu, Hiroki Sakaguchi and Gin-ya Adachi*
Department of Applied Chemistry, Faculty of Engineering, Osaka University, Yamadaoka, Suita, Osaka 565 (Japan)

Hiroyoshi Kanai
Faculty of Living Science, Kyoto Prefectural University, Shimogamo, Sakyoku, Kyoto 606 (Japan)

Satohiro Yoshida
Department of Hydrocarbon Chemistry and Division of Molecular Engineering, Kyoto University, Yoshida-honmachi, Sakyoku, Kyoto 606 (Japan)

(Received August 3, 1992)

Abstract

The local structure in hydrogenated amorphous $LaNi_{5.0}$ films was analysed by means of extended X-ray absorption fine structure. The short-range order in the amorphous $LaNi_{5.0}$ film was found to be little affected by the absorption of hydrogen. The lengthening of the interatomic distance with an increase in hydrogen concentration was much smaller for an amorphous film than for a crystalline bulk, so that the amorphous film appears to have excellent durability with regard to the hydrogen absorption–desorption process.

1. Introduction

Amorphous $LaNi_5$ films are potential materials for hydrogen storage and have many possibilities of application, such as hydrogen isotope separation, catalysis and negative electrodes for batteries [1–4]. It has been revealed that these films do not disintegrate into fine particles after repeated hydrogen absorption–desorption cycles, and absorb less than half the amount of hydrogen taken up by the crystalline bulk [5, 6]. The properties appear to be certainly related to structural differences between the amorphous and crystalline alloys. Although numerous studies [7–12] have been devoted to the correlation between the structure and hydrogen absorption properties of crystalline $LaNi_5$ alloy, almost nothing is known about the corresponding amorphous alloys. It is therefore interesting to perform structural studies of the amorphous films as a function of hydrogen content.

In our previous work associated with the amorphous $LaNi_5$ films using extended X-ray absorption fine structure (EXAFS) [13], an increase in the interatomic distance was observed in the amorphous film, though the environment of the Ni and La atoms in the amorphous film resembled that in the crystalline bulk. Thus, hydrogen sites in the amorphous film appear to be distorted in comparison with those in the crystalline bulk.

In this paper, we have investigated the change in local structures around the La and Ni atoms in the amorphous films with increasing hydrogen concentration by means of EXAFS, and discussed the relationship between the local structure and the hydrogen absorption characteristics.

2. Experimental details

The $LaNi_{5.0}$ amorphous films (about 1 μm thick) were deposited on a polyimide membrane (Kapton, 40 μm thick) at room temperature by means of the sputtering method [6, 14, 15]. The $LaNi_{5.0}$ crystalline powder and pure Ni foil were used as reference materials. The detailed procedure of preparation and characterization of prehydrogenated $LaNi_5$ samples has been described in a previous paper [13]. The procedure of activation to hydrogenate the sample was as follows. The samples prepared were transferred under an atmosphere of Ar gas (99.999%) into the stainless steel cell with X-ray transparent Kapton (75 μm thick, Toray - Du Pont Co., Ltd.) windows. A pressure of 1.0×10^6 Pa of H_2 (99.999%) was applied to the sample for 2 h at 363 K, then the cell was cooled to 273 K in an ice-bath

*Author to whom correspondence should be addressed.

0925-8388/93/$6.00

for 2 h, maintaining constant pressure. The heating–cooling process was repeated five times.

The measurements of the X-ray absorption spectra (XAS) were performed using synchrotron radiation employing the EXAFS facilities of BL-7C of the Photon Factory in the National Laboratory for High-Energy Physics, Tsukuba. The EXAFS spectra were collected at the Ni K edges and La L_{III} edges. The total thicknesses of the $LaNi_{5.0}$ films used for the X-ray absorption measurements were about 35 and 20 μm for the La and Ni edges respectively. The XAS data of the as-prepared samples were obtained *in vacuo* at 220 K, and those of the hydrogenated samples under constant pressures of 1.0×10^5 and 8.0×10^5 Pa at 220 K using the cell mentioned above. The hydrogen content in the $LaNi_5$ films was determined by a quartz crystal, mass monitoring (QCMM) method [6].

The EXAFS data were analysed with a 'KABO' program in the FACOM M382 computer system at the Data Processing Centre, Kyoto University [16]. The procedure for the extraction of EXAFS oscillations from the XAS and the determination of structural parameters were noted previously [13]. To obtain the radial structure function (RSF), Fourier transforms were performed over the range of 3.3–14.0 $Å^{-1}$ and 4.0–9.2 $Å^{-1}$ for the Ni and La edges respectively. To determine structural parameters, the main peaks (Ni 1.6–2.7 Å; La 2.4–3.4 Å) were Fourier filtered into the k space and the inverse Fourier transforms were analysed by the single scattering formula developed by Stern and others [17–19]. The resulting filtered EXAFS was fitted to the formula by means of the non-linear least-squares curve-fitting method, using theoretical phase shifts and backscattering amplitudes of Teo and Lee [20].

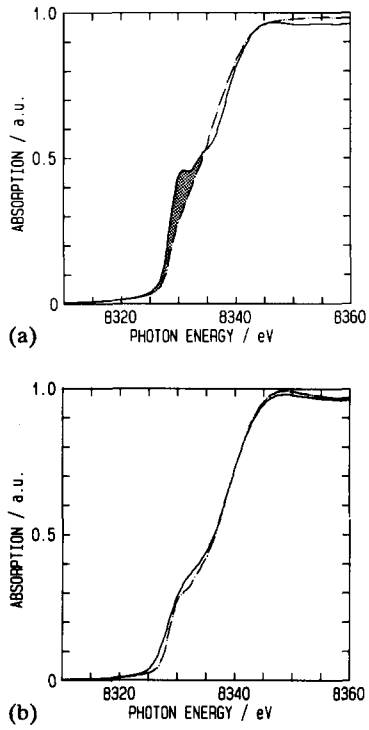

Fig. 1. Ni K edge XANES spectra for $LaNi_5$ (a) crystalline bulk and (b) amorphous film: ——, as-prepared; –·–·– hydrogenated (H_2 8.0×10^5 Pa).

3. Results and discussion

Figure 1(a) shows Ni K edge XANES spectra for $LaNi_{5.0}$ crystalline bulk and its hydride $LaNi_{5.0}H_7$. The Ni K near-edge spectrum is associated with the $l=1$(p-like) projected density of final states, and the shape of the absorption edge reflects the extent of Ni 3d–4p hybridization. The difference between the spectra is the decrease in area at the edge (shaded area), resulting from less 3d–4p hybridization owing to the narrowing of the Ni 3d band. Calculations [21] have shown that the Ni 3d bands narrow from 3.2 eV in $LaNi_5$ to less than 2.5 eV in $LaNi_5H_7$ partly because of the large lattice expansion upon hydrogenation. Garcia *et al.* [22] reported that, in the $CeFe_2$ system, the Fe K edge absorption peak at the absorption edge also decreased owing to hydrogenation, which can be attributed to the decrease in p–d mixing and corresponding increased 3d electrons localization. Another possible interpretation obtained from the calculation for the difference in the line shapes at the edge is the modification of the Ni d bands because of the formation of Ni–H bonding.

The shape of the absorption edge for the hydrogenated $LaNi_{5.0}$ amorphous film is almost the same as that for the as-prepared amorphous film as shown in Fig. 1(b). Therefore, it appears that hydrogen in the amorphous film does not affect the width of the Ni 3d band; *i.e.* the shape of the absorption edge, because a weakening 3d–4p hybridization had occurred with the amorphization of $LaNi_5$ [13].

Figures 2 and 3 show the k^3-weighted EXAFS spectra at Ni K edges and La L_{III} edges in the sputtered amorphous $LaNi_{5.0}$ films at various hydrogen contents. The magnitudes of the Fourier transforms obtained by a Fourier analysis of the EXAFS data in these films are also shown in Figs. 4 and 5. A large peak appeared on the Ni edge at about 2 Å, corresponding to mainly Ni–Ni and partially Ni–La distances, while on the La edge the peak appeared at about 3 Å, corresponding to the La–Ni distances. The profiles of the Fourier transforms in the hydrogenated samples show a resemblance to those in the as-prepared samples. Thus, it was suggested that the local structures around the central Ni and La atoms for the hydrogenated samples were similar to those for the as-prepared samples. The main peak height of the Fourier transforms, however,

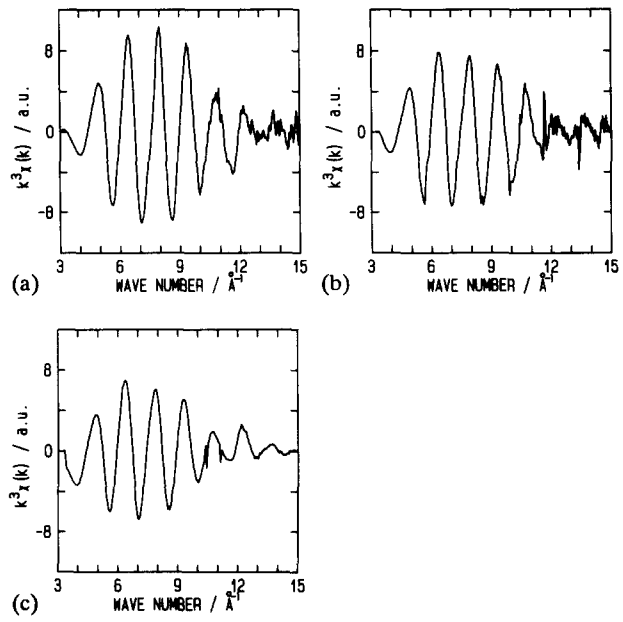

Fig. 2. Ni K edge k^3-weighted EXAFS spectra in (a) the as-prepared film and its hydrides (b) $LaNi_{5.0}H_{1.0}$ and (c) $LaNi_{5.0}H_{1.2}$.

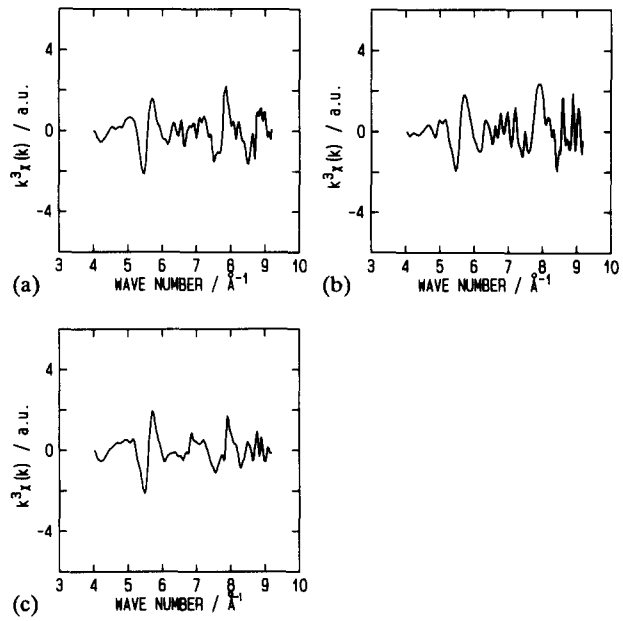

Fig. 3. La L_{III} edge k^3-weighted EXAFS spectra in (a) the as-prepared film and its hydrides (b) $LaNi_{5.0}H_{1.0}$ and (c) $LaNi_{5.0}H_{1.2}$.

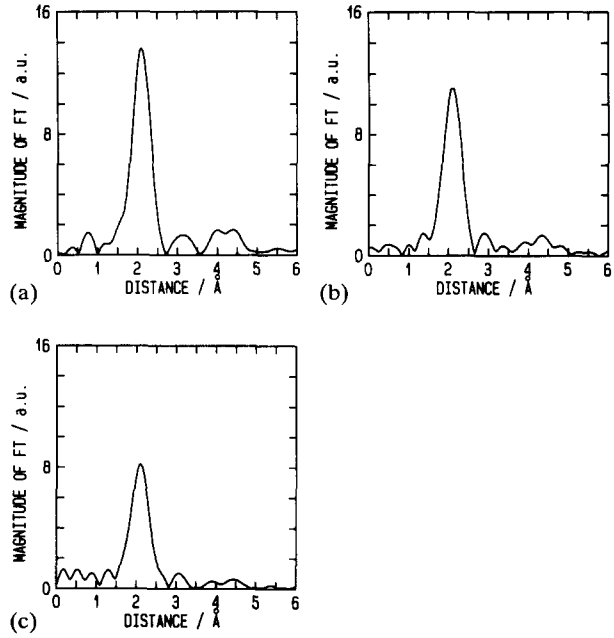

Fig. 4. Ni K edge RSF in (a) the as-prepared film and its hydrides (b) $LaNi_{5.0}H_{1.0}$ and (c) $LaNi_{5.0}H_{1.2}$.

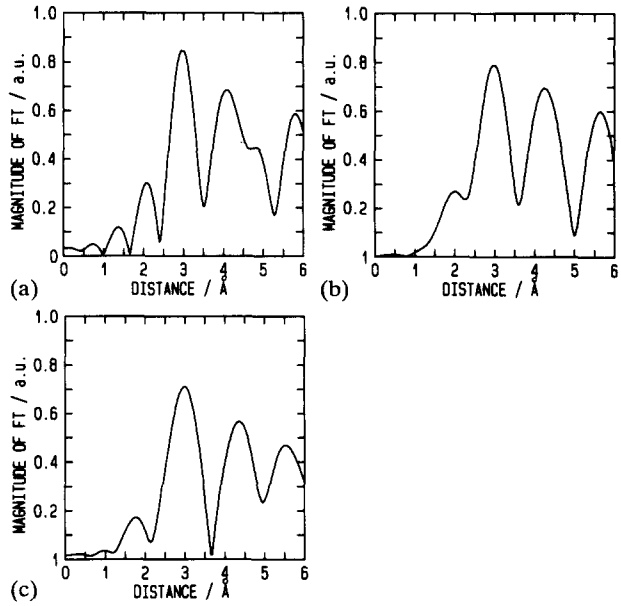

Fig. 5. La L_{III} edge RSF in (a) the as-prepared film and its hydrides (b) $LaNi_{5.0}H_{1.0}$ and (c) $LaNi_{5.0}H_{1.2}$.

decreases with increasing hydrogen concentration. The damping of the main peak for the hydrogenated samples is assumed to occur by either decreasing the coordination number or increasing the static disorder [23] induced by hydrogen.

The results of the curve fitting analysis on the Ni K edges and La L_{III} edges before and after hydrogenation are presented in Tables 1 and 2. There are two kinds of Ni atoms with different symmetry in the $LaNi_5$ crystalline bulk, *i.e.* Ni_I atoms (coordination number 6) and Ni_{II} atoms (coordination number 4). From the previous EXAFS study of as-prepared $LaNi_{5.0}$ films [13], it has been seen that the main peak in Ni radial structure function (RSF) contains information on two subshells of Ni–Ni pairs (Ni_I–Ni_{II}, Ni_{II}–Ni_{II}) and one subshell of an Ni–La(Ni_I–La) pair, whereas the peak in La RSF is related to two subshells of La–Ni pairs (La–Ni_I, La–Ni_{II}). These subshells were also adopted to analyse the hydrogenated samples.

The coordination number of each subshell for the as-prepared film was almost the same as that for the

TABLE 1. Structural parameters at the Ni K edge for $LaNi_{5.0}$ amorphous film and its hydrides

N	L(Å)	σ^2 (Å$^2\times10^{-3}$)	R
As-prepared film			
4.6Ni±0.5	2.46±0.01	6.8	
3.5Ni±0.9	2.57±0.02	13.2	4.8×10^{-3}
1.7La±1.4	2.92±0.08	14.6	
Hydrogenated film ($LaNi_{5.0}H_{1.0}$)			
4.6Ni±0.6	2.47±0.01	7.6	
3.5Ni±1.2	2.60±0.02	14.3	7.2×10^{-3}
1.7La±1.7	2.94±0.10	15.9	
Hydrogenated film ($LaNi_{5.0}H_{1.2}$)			
4.6Ni±0.5	2.47±0.01	8.6	
3.6Ni±0.9	2.61±0.02	13.2	5.4×10^{-3}
1.8La±1.4	2.95±0.08	17.5	

N real coordination number [13]; L interatomic distance; σ Debye–Waller factor; $R=(\{\Sigma_k[\chi_{obs}(k)-\chi_{calc}(k)]^2\}/[\Sigma_k\chi_{obs}(k)]^2)^{1/2}$.

TABLE 2. Structural parameters at the La L_{III} edge for $LaNi_{5.0}$ amorphous film and its hydrides

B	L (Å)	σ^2 (Å$^2\times10^{-2}$)	R
As-prepared film			
1.3Ni±0.1	3.01±0.01	2.1	
2.8Ni±0.2	3.27±0.01	2.1	6.6×10^{-3}
Hydrogenated film ($LaNi_{5.0}H_{1.0}$)			
1.5Ni±0.2	3.03±0.02	2.4	
2.7Ni±0.3	3.31±0.02	2.0	5.7×10^{-3}
Hydrogenated film ($LaNi_{5.0}H_{1.2}$)			
1.6Ni±0.2	3.05±0.02	2.5	
2.8Ni±0.2	3.30±0.02	2.2	5.4×10^{-3}

B apparent coordination number; L interatomic distance; σ Debye–Waller factor; $R=(\{\Sigma_k[\chi_{obs}(k)-\chi_{calc}(k)]^2\}/[\Sigma_k\chi_{obs}(k)]^2)^{1/2}$.

hydrogenated samples within the experimental error, and the interatomic distance of each subshell increased with the hydrogen concentration. Since the coordination number remained unchanged, the decrease in peak height observed for the hydrogenated films compared with that for the as-prepared films (as shown in Figs. 4 and 5) is due solely to an increase in the Debye–Waller factor. The EXAFS study on hydrogenation of Pd clusters supported on Al_2O_3 showed that the increase in the Debye–Waller factor for the hydrogenated sample indicates the structural disorder due to the interstitial hydrogen [24].

It is well known that the interatomic distance in the $LaNi_5$ crystalline bulk increases owing to the phase transformation from the α to β phase. This generates microcracks and then the alloy is pulverized. The crystal structure of the α phase has been studied by Soubeyroux *et al.* [10] and that of the β phase by Lartigue and coworkers [7, 9] by means of powder neutron diffraction. Figure 6 illustrates the dependence of the hydrogen concentration on the interatomic distance in the amorphous film and the crystalline bulk, using the example of an Ni_I–Ni_{II} pair. For the crystalline bulk, the β phase appears at about 0.4H/$LaNi_5$. Subsequently, the sudden increase in the Ni_I–Ni_{II} distance is observed at this hydrogen concentration [10]. The increase in the Ni_I–Ni_{II} interatomic distance with hydrogen concentration for the amorphous film was in agreement with that for the α phase in the crystalline bulk, and the tendency was maintained up to 1.2H/$LaNi_5$. This appears to be one of the reasons why amorphous films do not pulverize.

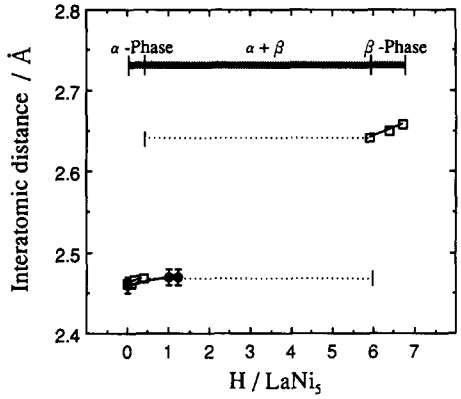

Fig. 6. Hydrogen concentration dependence of the Ni_I–N_{II} interatomic distance: □, crystalline bulk; ●, amorphous film.

The differences in the mechanism of phase transformation between the amorphous film and the crystalline bulk can be attributed to the differences in the process of occupation of hydrogen sites. EXAFS analyses have shown the similarity of the short-range order between the amorphous film and the crystalline bulk [13]. Therefore, the hydrogen sites with the same structure as D1, D3 and D5 sites in the crystalline bulk proposed by Lartigue *et al.* [9] appear to exist also in the amorphous film.

Absorbing hydrogen, the crystalline bulk forms an α phase where a portion of the D5 sites are occupied by hydrogen up to 0.4H/$LaNi_5$. Also, a β phase is formed with large lattice expansion when more hydrogen atoms enter some of the D1 or D3 sites; in particular, when D1 sites are occupied this causes a displacement of the Ni_I atoms in the c direction and a further increase in the Ni_I–Ni_{II} interatomic distances [8]. In the case of the amorphous film, some of the D5 sites may be occupied by hydrogen up to 1.2H/$LaNi_5$, whereas the D1 and D3 sites remain unoccupied, so that the increase in the Ni_I–Ni_{II} interatomic distance appears to be relatively small. For the above reasons, amorphous films exhibited excellent durability to the hydrogen absorption–desorption cycling process in comparison with that of the crystalline bulk.

4. Conclusions

The local structures around the La and Ni atoms in amorphous $LaNi_5$ films and their hydrides have been clarified with EXAFS. The hydrogen-induced increase in the distance of the Ni_I–Ni_{II} pairs for the amorphous film was found to be consistent with that for the α phase in the crystalline bulk, and this appears to prevent the amorphous films from pulverizing.

Acknowledgments

We thank Dr. M. Nomura and the staff of the Photon Factory at KEK for their helpful advice and technical assistance in the EXAFS measurements. This work was partially supported by Grants in Aid for Scientific Research Nos. 03750581 and 04750693 for H. Sakaguchi, from the Ministry of Education, Science and Culture. This work has been performed under the approval of the Photon Factory Programme Advisory Committee (Proposal No. 90–151).

References

1 G. Adachi, H. Nagai and J. Shiokawa, *J. Less-Common Met., 97* (1984) L9.
2 H. Sakaguchi, G. Adachi and J. Shiokawa, *Bull. Chem. Soc. Jpn., 61* (1988) 521.
3 H. Sakaguchi, Y. Yagi, J. Shiokawa and G. Adachi, *J. Less-Common Met., 149* (1989) 185.
4 T. Sakai, H. Ishikawa, H. Miyamura, N. Kuriyama, S. Yamada and T. Iwasaki, *J. Electrochem. Soc., 138* (1991) 908.
5 H. Sakaguchi, N. Taniguchi, H. Nagai, K. Niki, G. Adachi and J. Shiokawa, *J. Phys. Chem., 89* (1985) 5550.
6 H. Sakaguchi, H. Seri and G. Adachi, *J. Phys. Chem., 94* (1990) 5313.
7 C. Lartigue, A. Percheron-Guegan, J. C. Achard and J. L. Soubeyroux, *J. Less-Common Met., 113* (1985) 127.
8 P. Thompson, J. J. Reilly, L. M. Corliss, J. M. Hastings and R. Hempelmann, *J. Phys. F, 16* (1986) 675.
9 C. Lartigue, A. Le Bail and A. Percheron-Guegan, *J. Less-Common Met., 129* (1987) 65.
10 J. L. Soubeyroux, A. Percheron-Guegan and J. C. Achard, *J. Less-Common Met., 129* (1987) 181.
11 D. Noreus, L. G. Olsson and P.-E. Werner, *J. Phys. F, 13* (1983) 715.
12 R. Hempelmann, D. Richter, G. Eckold, J. J. Rush, J. M. Rowe and M. Montoya, *J. Less-Common Met., 104* (1984) 1.
13 T. Suenobu, H. Sakaguchi, T. Tsuji, H. Kanai, S. Yoshida and G. Adachi, *Bull. Chem. Soc. Jpn., 64* (1991) 3522.
14 G. Adachi, H. Sakaguchi, K. Niki, H. Nagai and J. Shiokawa, *Bull. Chem. Soc. Jpn., 58* (1985) 885.
15 H. Sakaguchi, N. Taniguchi, H. Seri, J. Shiokawa and G. Adachi, *J. Appl. Phys., 64* (1988) 888.
16 B. J. Tan, H. J. Klabunde, T. Tanaka, H. Kanai and S. Yoshida, *J. Am. Chem. Soc., 110* (1988) 5951.
17 E. A. Stern, *Phys. Rev. B., 10* (1974) 3027.
18 C. A. Ashley and S. Doniach, *Phys. Rev. B, 11* (1975) 1279.
19 P. A. Lee and J. B. Pendry, *Phys. Rev. B., 11* (1975) 2795.
20 B. K. Teo and P. A. Lee, *J. Am. Chem. Soc., 101* (1979) 2815.
21 M. Gupta, *J. Less-Common Met., 130* (1987) 219.
22 J. Garcia, J. Bartolome, M. Sanchez del Rio, A. Marcelli, D. Fruchart and S. Miraglia, *Z. Phys. Chem., 163* (1989) 279.
23 B. K. Teo, *EXAFS: Basic Principles and Data Analysis*, Springer, Berlin, 1986, p. 34.
24 R. J. Davis, S. M. Landry, J. A. Horsley and M. Boudart, *Phys. Rev. B, 39* (1989) 10580.